JOURNAL OF SOLID STATE CHEMISTRY 98, 11–24 (1992)

Synthesis, X-Ray Single Crystal Structure Determination, and Dehydration Study of $BaZr_2F_{10} \cdot 2H_2O$ by X-Ray Powder Thermodiffractometry

Y. GAO, J. GUERY, A. LE BAIL, AND C. JACOBONI*

Laboratoire des Fluorures—URA CNRS 449, Faculté des Sciences—Université du Maine, 72017 Le Mans Cedex, France

Received June 6, 1991; in revised form October 3, 1991

Single crystals of $BaZr_2F_{10} \cdot 2H_2O$ were prepared from BaF_2–ZrF_4 mixtures in aqueous HCl solution. The crystal structure has been solved in the orthorhombic *Pnam* space group: $a = 7.8974(3)$ Å, $b = 7.9076(3)$ Å, $c = 14.7227(4)$ Å, $R_F = 0.017$, and $R_I = 0.023$ from a twinned crystal whose apparent space group was $P4_22_12$. The bidimensional structure is built up from infinite corner-sharing in the (001) plane of $[Zr_2F_{14}]^{6-}$ bipolyhedra formed by edge-sharing of two $[ZrF_8]^{4-}$ trigonal dodecahedra; between each $[Zr_2F_{10}]^{2-}$ layer, Ba atoms and H_2O molecules ensure the cohesion of the structure. The dehydration process has been studied by TGA and X-ray thermodiffractometry; at 130°C the first H_2O molecule reversibly leaves without damaging the crystal structure which becomes isotypic to that of $TlZrF_5$; above 150°C the second H_2O molecule continuously leaves up to 210°C, where the crystal structure collapses.

Introduction

The phase diagram of the BaF_2–ZrF_4 system was investigated by Laval *et al.* (*1–4*) by means of solid state reactions. The knowledge of properties of this binary system is of great interest since BaF_2 and ZrF_4 are the major components of the fluoride glass ZBLAN family. For instance, β-$BaZrF_6$ and α, β-$BaZr_2F_{10}$ have been identified in the crystallization process studies of ZBLAN glasses (*5–7*); these last three compounds also serve as reference materials in the investigation of the glass structure (*8*).

A difficult problem concerns the chemical analysis of metallic traces in such ZBLAN glasses at the sub-ppm level; it is necessary to dissolve the glass; in most cases HCl solution is used for chemical attack under microwave heating of the sample placed in a Teflon bomb. Because of the low solubility of some components of the glass, part of the degraded sample remains solid; X-ray powder diffractometry characterization has shown that the solid phase is a complex mixture.

The aim of the present work was to obtain a better understanding of the ZBLAN properties in such a HCl medium. We have therefore studied the reaction of BaF_2 and ZrF_4 in HCl. These experiments have been extended to the BaF_2–HfF_4 system since, from the crystallographic point of view, HfF_4 can be easily substituted for ZrF_4. The thermal

* To whom correspondence should be addressed.

0022-4596/92 $5.00

TABLE I

CHEMICAL ANALYSIS OF $BaZr_2F_{10} \cdot 2H_2O$

	Ba	Zr	F	H_2O
Weight %	24.8	34.6	33.9	6.7
Molar ratio	1	2.04	9.9	2.1

Note. H_2O content is deduced from other values.

behavior of the new phase $BaZr_2F_{10} \cdot 2H_2O$ has been studied by X-ray thermodiffractometry.

Crystal Preparation in the BaF_2–ZrF_4 System

The compounds are prepared under hydrothermal condition from 0.5 g mixture of powders of BaF_2 and ZrF_4 in 4 ml of hydrochloric acid solutions (6 *M*); the reactants are introduced in an hermetic Teflon jar which is placed in a metallic container (PARR or BERGHOF bomb). The materials are heated at 200°C for 3 days (the estimated pressure is 200 bars) and then cooled, either by switching off the heating source or at a controlled cooling rate of 0.05°C/min.

Crystals can also be formed from the same starting mixture in a Teflon beaker heated in a sand bath at 150°C for 3 hr; the powder does not dissolve entirely; by natural cooling to room temperature well-shaped crystals are obtained.

Two types of crystals are found, depending on the starting composition.

—One phase is obtained in platelets and is identified by X-ray powder diffraction as γ-$BaZrF_6$, which had been recently synthesized and characterized, using similar hydrothermal conditions (but in HF solution) (*9*).

—The other phase crystallizes in a rhombic shape; the chemical analysis of Ba and Zr by ICP–AES and F by pyrohydrolysis of fluorine leads to the experimental composition (Table I); since no chlorine was detected, the remaining 6.7% weight composition is attributed to H_2O molecules; the chemical formula then is $BaZr_2F_{10} \cdot 2H_2O$.

The nature of the crystals formed from the various starting composition is shown in Fig. 1. The Ba content in solid phases is always higher than in the starting fluoride mixture: this characterizes the higher solubility of ZrF_4; $BaZr_2F_{10} \cdot 2H_2O$ which seems to be the more stable phase in these conditions can be obtained pure from the BaF_2–$2ZrF_4$ mixture in the sand bath or in the PARR bomb from a mixture richer in ZrF_4 (10BaF_2–90ZrF_4 in mole%).

Crystal Structure Determination of $BaZr_2F_{10}$, $2H_2O$

The colorless crystal selected for X-ray measurements on a Siemens AED-2 four-circle diffractometer was limited by the (100), (010), and (001) faces. Experimental details are given in Table II.

The conditions limiting reflections led un-

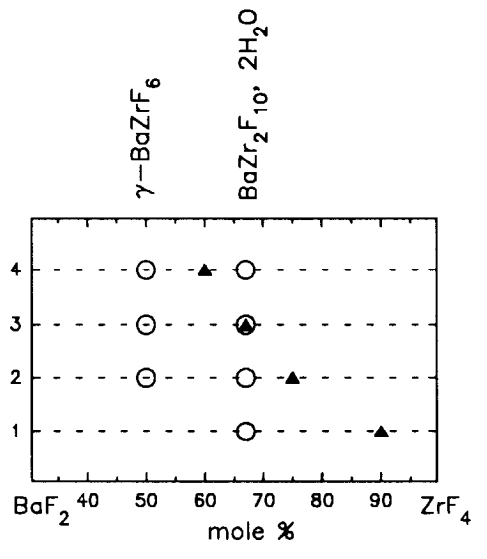

FIG. 1. Main crystallized phases (○) formed in the BaF_2–ZrF_4 system from various starting compositions (▲).

TABLE II

CELL PARAMETERS (Å) AND CONDITIONS OF DATA COLLECTION AND TREATMENT FOR $BaZr_2F_{10} \cdot 2H_2O$

Tetragonal pseudo-cell	
Apparent space group	$P4_22_12$
Cell parameters refined from 36 reflections in the range 15°–16°θ	a = 7.900(2) Å, c = 14.723(6) Å
Crystal size	0.05 × 0.05 × 0.14 mm^3
Radiation	Mo$K\alpha$
Detector aperture (mm)	3.5 × 3.5
Data range, $2\theta_{min}$–$2\theta_{max}$	1°–70°
Scan type	ω-2θ
hkl_{min}, hkl_{max}	$\bar{1}3\ 0\ 0/12\ 11\ \bar{1}9$
Standard reflections	$6\ 0\ 2/0\ 6\ 2/\bar{1}\ 4\ \bar{8}$
Reflections measured	1773
Unique reflections merged in 4/*mmm*	1044
R_{av}	0.030
Data retained ($I > 3\sigma_{(I)}$)	947
Linear absorption coefficient	μ = 65.7 cm^{-1}
Absorption correction (Gauss method)	T_{min} = 0.714, T_{max} = 0.744
Orthorhombic true cell of the twinned crystal	
Space group	*Pnam*
Cell parameters (from X-ray powder data)	a = 7.8974(3) Å, b = 7.9076(3) Å, c = 14.7227(4) Å, V = 919.4 Å^3; Z = 4; M = 545.75 g · mole^{-1}
Calculated density	3.942
Unique reflections	1000
Data retained ($I > 3\sigma_{(I)}$)	940
Parameters refined	74
No extinction correction; the two most intense reflections (004 and 008) are excluded	
Agreement factors	$R_F = \frac{\Sigma\|\|F_0\| - k\|F_c\|\|}{\Sigma\|F_0\|} = 0.017$, $R_I = \frac{\Sigma\|I_0 - kI_c\|}{\Sigma I_0} = 0.023$
X-ray powder data	
Diffractometer	Siemens D500–DACO MP
Radiation	Cu$K\alpha$, graphite monochromator in the reflected beam
2θ range	10°–130° (2θ)
Step scan	0.03° (2θ)
Data used in Rietveld refinement	20°–130° (2θ)
Number of reflections	811
Pseudo-Voigt profile shape	η = 0.67(1)
Half-width parameters U, V, W	0.064(8), −0.018(8), 0.038(2)
Bragg R factor	0.057
R_F factor	0.031
Conventional Rietveld profile factors	R_p = 0.111, R_{wp} = 0.142

TABLE IIIA

ATOMIC COORDINATES AND ISOTROPIC TEMPERATURE FACTORS

$$B_{eq} = \frac{4}{3}\sum_i \sum_j b_{ij} \cdot (\mathbf{a}_i \cdot \mathbf{b}_j) \quad (19)$$

Atom	Site	x	y	z	B_{eq}
Ba	4c	0.12239(5)	0.09033(5)	$\frac{1}{4}$	1.29(1)
Zr	8d	0.33317(5)	0.33639(5)	−0.00145(3)	0.53(2)
F(1)	8d	0.0058(3)	0.0095(3)	0.0794(1)	1.01(9)
F(2)	8d	0.0616(4)	0.2886(4)	−0.0022(2)	1.86(11)
F(3)	8d	0.2872(4)	0.0663(3)	−0.0165(2)	1.48(10)
F(4)	8d	0.2935(4)	0.2697(4)	0.1284(2)	2.01(12)
F(5)	8d	0.2732(5)	0.3237(4)	0.8654(2)	2.16(12)
O(1)	4c	0.3324(7)	0.5923(7)	$\frac{1}{4}$	2.55(22)
O(2)[a]	8d	0.5031(9)	0.0602(9)	0.2259(5)	2.93(38)

Note. e.s.d.'s are in parentheses.

[a] The O(2) site is half occupied.

ambiguously to the $P4_22_12$ space group (No. 94). Application of the direct method facilities of the SHELS-86 program (*10*), to a 1 Å resolution limited data set, provided starting coordinates for the Ba and Zr atoms and for a part of the fluorine atoms. Scattering factors for Ba^{2+}, Zr^{4+}, and F^- ions were taken from the "International Tables for X-Ray Crystallography" (*11*) and for O^{2-} from Ref. (*12*). Successive refinements and Fourier difference synthesis, using the SHELX76 program (*13*), led to a structure with a fully credible crystal chemistry, if one ignored the fact that the Ba atom occupied half its site. At this stage, the formulation was $BaZr_2F_{10} \cdot H_2O$ (a water molecule was missing) and the residual stabilized to R = 0.26 in the isotropic thermal motion approximation. All attempts to improve this result were unsuccessful in tetragonal symmetry.

Possible twinning was suspected when a careful examination of the raw intensity data

TABLE IIIB

ANISOTROPIC THERMAL PARAMETERS $U_{ij} \times 10^4$

Atom	U_{11}	U_{22}	U_{33}	U_{23}	U_{13}	U_{12}
Ba	225(2)	158(2)	108(1)	0	0	−83(1)
Zr	63(2)	26(2)	113(2)	5(1)	0(1)	−3(1)
F(1)	142(12)	120(11)	122(10)	4(8)	−10(8)	36(6)
F(2)	74(11)	68(10)	566(21)	7(11)	−1(13)	−6(8)
F(3)	118(12)	49(10)	397(16)	1(10)	7(11)	−19(9)
F(4)	345(18)	230(15)	187(13)	50(12)	68(13)	−129(12)
F(5)	394(17)	254(14)	173(14)	18(12)	−94(13)	−150(13)
O(1)	449(32)	254(26)	267(25)	0	0	196(25)
O(2)	247(32)	407(42)	460(69)	0	0	−29(31)

Note. The vibrational coefficients relate to the expression $T = \exp(-2\pi^2(h^2a^{*2}U_{11} + k^2b^{*2}U_{22} + l^2c^{*2}U_{33} + 2klb^*c^*U_{23} + 2hla^*c^*U_{13} + 2hka^*b^*U_{12}))$.

TABLE IV

SELECTED BOND LENGTHS (Å) AND ANGLES (°)

Zr polyhedron ⟨Zr–F⟩ = 2.110 Å

Zr	F(4)	F(5)	F(2)	F(3)	F(3)	F(2)	F(1)	F(1)
F(4)	**2.008(2)**	3.899(5)	2.897(4)	2.936(3)	2.672(4)	2.660(4)	2.526(4)	3.933(2)
F(5)	151.0(3)	**2.019(3)**	3.127(4)	2.976(3)	2.679(4)	2.582(4)	3.878(3)	2.422(4)
F(2)	90.9(3)	100.2(3)	**2.057(3)**	3.942(4)	2.461(4)	3.996(4)	2.551(4)	2.671(4)
F(3)	92.1(2)	93.4(2)	145.7(2)	**2.069(2)**	4.027(4)	2.515(4)	2.563(3)	2.671(3)
F(3)	79.2(3)	79.2(3)	71.0(3)	143.0(2)	**2.178(2)**	2.512(4)	4.028(2)	3.977(3)
F(2)	78.8(3)	75.8(3)	141.3(2)	72.6(3)	70.4(3)	**2.178(3)**	4.037(3)	4.002(3)
F(1)	74.0(3)	134.7(2)	73.9(3)	74.1(2)	135.0(2)	135.6(2)	**2.182(2)**	2.345(2)
F(1)	138.8(1)	70.1(3)	77.8(2)	77.6(2)	131.0(2)	132.6(2)	64.8(2)	**2.193(2)**

Ba environment		O(1) environment		O(2) environment	
2 × Ba–F(4)	2.654(3)	2 × O(1)–F(5)	2.633(5)	O(2)–F(4)	2.747(11)
Ba–O(1)	2.708(6)	O(1)–Ba	2.707(5)	O(2)–O(1)	2.888(9)
2 × Ba–F(1)	2.750(2)	O(1)–O(2)	2.888(9)	O(2)–Ba	2.941(8)
2 × Ba–F(5)	2.831(3)	2 × O(1)–F(1)	2.972(3)	O(2)–F(4)	3.021(7)
Ba–O(2)	2.941(7)	2 × O(1)–F(4)	3.131(5)	O(2)–Ba	3.037(8)
Ba–O(2)	3.037(8)			O(2)–F(5)	3.173(10)
2 × Ba–F(4)	3.343(3)			O(2)–F(4)	3.176(10)
		F(5)–O(1)–F(5)	80.4(2)	F(4)–O(2)–O(1)	149.2(3)
				Ba–O(2)–Ba	103.3(3)

Zirconium–zirconium linkage

Edge		Zr–Zr	3.693(1)	Zr–F(1)–Zr	115.2(1)
Corners	2 ×	Zr–Zr	4.166(1)	Zr–F(3)–Zr	157.8(2)
	2 ×	Zr–Zr	4.178(1)	Zr–F(2)–Zr	161.3(2)

Note. e.s.d.'s are in parentheses.

revealed a curious condition on the observed reflections which did not match any of the diffraction symbols: in addition to the $00l : l = 2n$ and $h00 : h = 2n$ of the $P4_22_12$ space group, the $0kl$ reflections were not observed when k was odd *and* l even. We did not find any explanation for this phenomenon based on the tetragonal symmetry either in the $4/mmm$ Laue symmetry or by lowering it to $4/m$. We then considered the possibility that the crystal could have the orthorhombic symmetry with $a \approx b$ and could consist, on the average, of two domains (A and B) related by a 90° rotation around the common $\vec{c}$ axis, leading to a systematic overlap of the hkl(A) and khl(B) reflections. The volumes of the two domains would then have to be almost equal in order to explain the $R_{av} = 0.030$ obtained when fitting the data to $4/mmm$. Among all the orthorhombic space groups, only one centric space group could fulfill the above extinction requirements: *Pnam* (a nonstandard setting of the *Pnma* space group No. 62) with the conditions $h0l : h = 2n$ and $0kl : k + l = 2n$; one can easily verify that when h and k are mixed by the twinning effect, the existence conditions for the $0kl$ reflections are

—if $k = 2n$, then $l = 2n$ or $l = 2n + 1$
—if $k = 2n + 1$, then $l = 2n + 1$.

Disregarding temporarily the only other possibility corresponding to the associated $Pna2_1$ acentric space group, we could easily describe the previous structure in the *Pnam* space group; the site which was half-occupied by the Ba atoms in the $P4_22_12$ description led to two independent 4*c* sites in *Pnam*

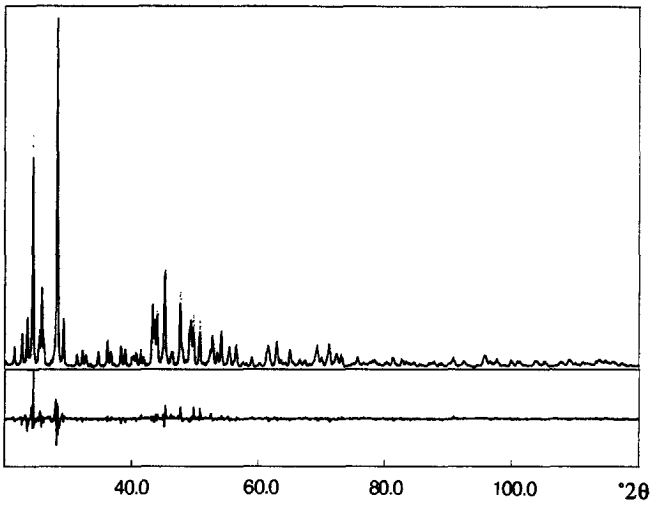

FIG. 2. Experimental (···) and calculated (—) powder X-ray diffraction patterns for $BaZr_2F_{10} \cdot 2H_2O$; the difference pattern is below at the same scale.

that we could then attribute, respectively, to a full Ba atom site and to the missing water molecule (or vice versa), confirming the expected $BaZr_2F_{10} \cdot 2H_2O$ formulation.

For the final calculations, we have used a local program (*14*) (previously applied in Refs. (*15–18*) to various twinning problems), where the minimal function was $\chi^2 = \Sigma\omega_i(I_0 - kI_c)^2$, assuming in the first step identical volumes with $I_c = F^2_{hkl_A} + F^2_{khl_B}$, $\omega_i = \dfrac{1}{I_0}$ (weighting scheme), where k is the scale factor. By testing the two possibilities of permutation between the Ba atom and the "missing" water molecule (O(2) in the following), the refinements clearly indicated the best configuration, leading to the residuals $R_F = 0.064$ ($R_I = 0.083$) with isotropic temperature factors and further to $R_F = 0.017$ ($R_I = 0.023$) when applying anisotropic thermal motion. A test applied to data not merged in 4/*mmm* Laue symmetry, to refine the individual volumes of the two domains, did not improve this result, nor did an attempt to use the $Pna2_1$ acentric space group. Finally, as O(2) was characterized by an enormous thermal motion along the c direction ($U_{33} = 0.23(1)$), its z coordinate was allowed to vary, leading to more reasonable thermal parameters (the constraints on U_{ij} for the 4*c* site were kept) without a change of the final residuals (940 reflections,

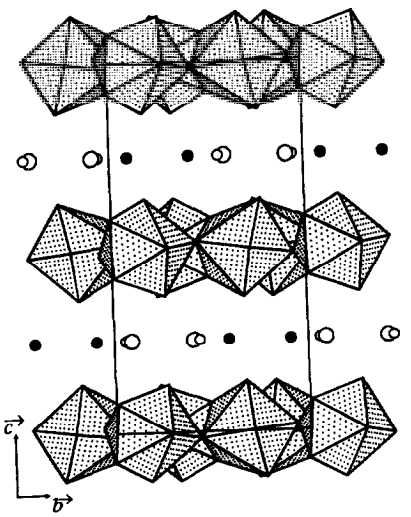

FIG. 3. Perspective view of the crystal structure of $BaZr_2F_{10} \cdot 2H_2O$. Large open circles are Ba^{2+} ions and small open circles are H_2O molecules. O(1) is symbolized by closed circles.

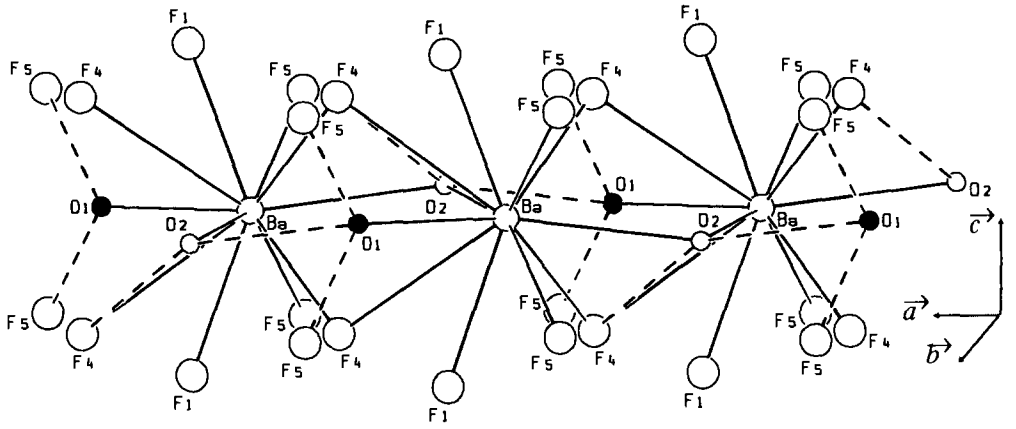

FIG. 4. Description of the interlayer environment in $BaZr_2F_{10} \cdot 2H_2O$. Large open circles are for F^-, medium sized open circles are for Ba^{2+} ions, and small circles are for H_2O molecules.

74 parameters). Thus, it seems that a static disorder characterizes O(2), and it is proposed that this unit half occupies a general position instead of the 4*c* site $(x,y,\frac{1}{4})$. The atomic coordinates and thermal motion parameters are given in Tables IIIA and IIIB; the main interatomic distances and angles are listed in the Table IV. The I_{obs}/I_{cal} list can be obtained on request to the authors.

In order to try to distinguish the values of the *a* and *b* cell parameters, we used X-ray powder data (grounded crystals) and the Rietveld method (*20*). The atomic coordinates from the single crystal data investigation were kept fixed during the refinement of the cell parameters and of the profile parameters and thermal motion factors using the DBW3.2S program (*21, 22*). When *a* was forced to be equal to *b*, one obtained *a* = 7.9028(2) Å and the conventional Rietveld

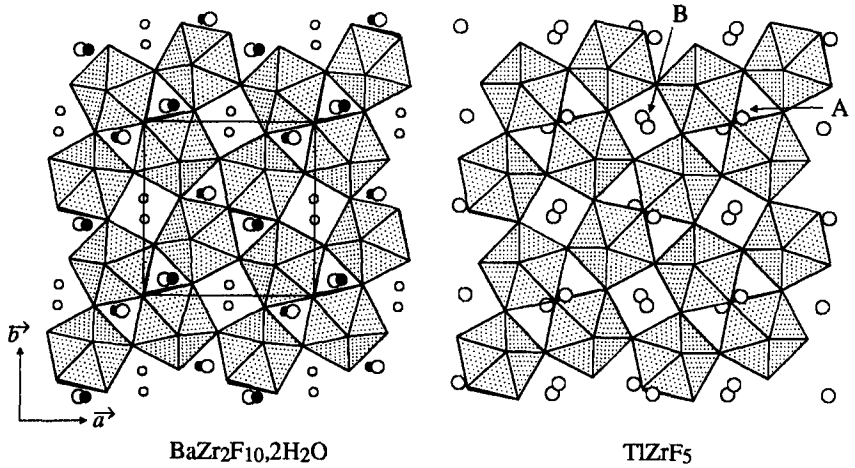

FIG. 5. Comparison of $[Zr_2F_{10}]^{2-}$ layers and cavity occupancies between $BaZr_2F_{10} \cdot 2H_2O$ (O(1) is symbolized by closed circles) and $TlZrF_5$.

TABLE V

VALENCE-BOND ANALYSIS OF $BaZr_2F_{10} \cdot 2H_2O$

	Ba	Zr	Sum	Expected
F(1)	0.21(*0.25*)(×2)	0.41(*0.44*) 0.40(*0.42*)	1.02(*1.11*)	1.
F(2)		0.57(*0.48*) 0.42(*0.48*)	0.99(*0.96*)	1.
F(3)		0.55(*0.68*) 0.42(*0.36*)	0.97(*1.04*)	1.
F(4)	0.27(*0.30*)(×2) 0.05(*0.09*)(×2)	0.64(*0.43*)	0.96(*0.82*)	1.
F(5)	0.17(*0.21*)(×2)	0.62(*0.79*)	0.79(*1.00*)	1.
O(1)	0.32		0.32	2.
O(2)	0.18(*0.23*) 0.14(*0.08*)		0.32(*0.31*)	2.
Sum	2.04(*2.01*)	4.03(*4.08*)		
Expected	2.0	4.0		

Ba–F $s = 0.25 \exp[(2.685-d_i)/0.391]$ (*24*)

Zr–F $s = \exp[(1.83-d_i)/0.4]$ (*25*)

Ba–O $s = (d_i/2.297)^{-7}$ (*26*)

Note. Corresponding values for $BaZr_2F_{10} \cdot H_2O$ are in italics.

reliabilities $R_I = 0.059$ and $R_p = 0.117$ (unweighted background-corrected peak-only agreement index); a slight improvement was obtained by allowing a and b to vary independently, leading to $R_I = 0.057$ and $R_p = 0.111$. Although the difference is small, we were convinced that this result is meaningful (the e.s.d.'s are, however, certainly underestimated) as judged by the examination at large angles (>100° 2θ) of the X-ray pattern, where the discrepancy between the final a and b values (≈0.01 Å) produces clear effects. Interatomic distances were calculated from these parameters listed in Table II. The experimental and calculated patterns are displayed in Fig. 2.

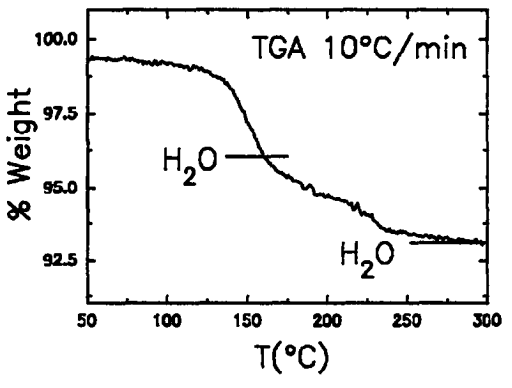

FIG. 6. TGA curve for $BaZr_2F_{10} \cdot 2H_2O$.

BaF_2–HfF_4 System

In the BaF_2–HfF_4 system, under the same conditions of preparation, isotypic crystals of $BaHf_2F_{10} \cdot 2H_2O$ were obtained; the compound was identified by comparing the shape of the crystals and their X-ray diffraction powder spectra which are similar to that of the zirconium compound. No Rietveld refinement was performed because it was not possible to obtain a pure phase; as expected, the cell parameters of equivalent phases with Zr and Hf are very close (for $BaHf_2F_{10} \cdot 2H_2O$: $a = 7.850(3)$ Å, $b = 7.856(3)$ Å, $c = 14.719(2)$ Å).

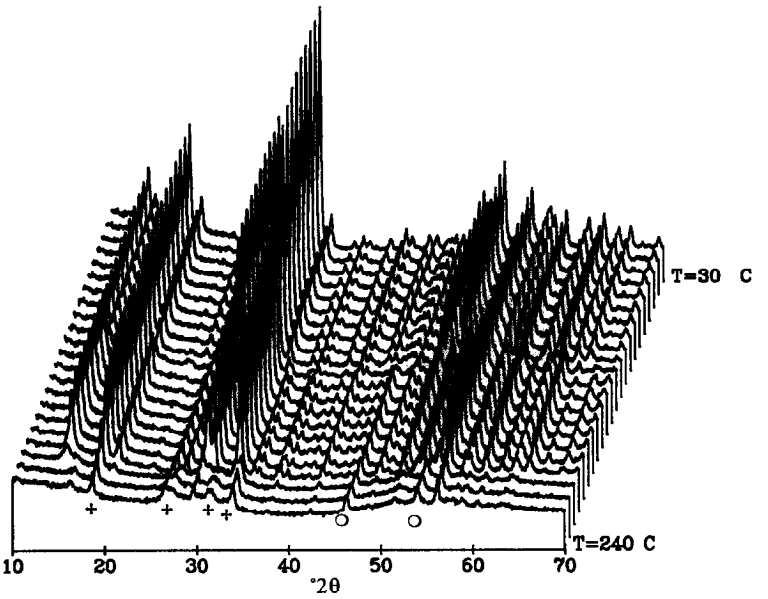

FIG. 7. 10°–70°(2θ) part of the powder X-ray thermodiffractogram for $BaZr_2F_{10} \cdot 2H_2O$ (O marks correspond to platinum foil lines due to heat cracking of the sample surface and + marks to ZrF_4 lines).

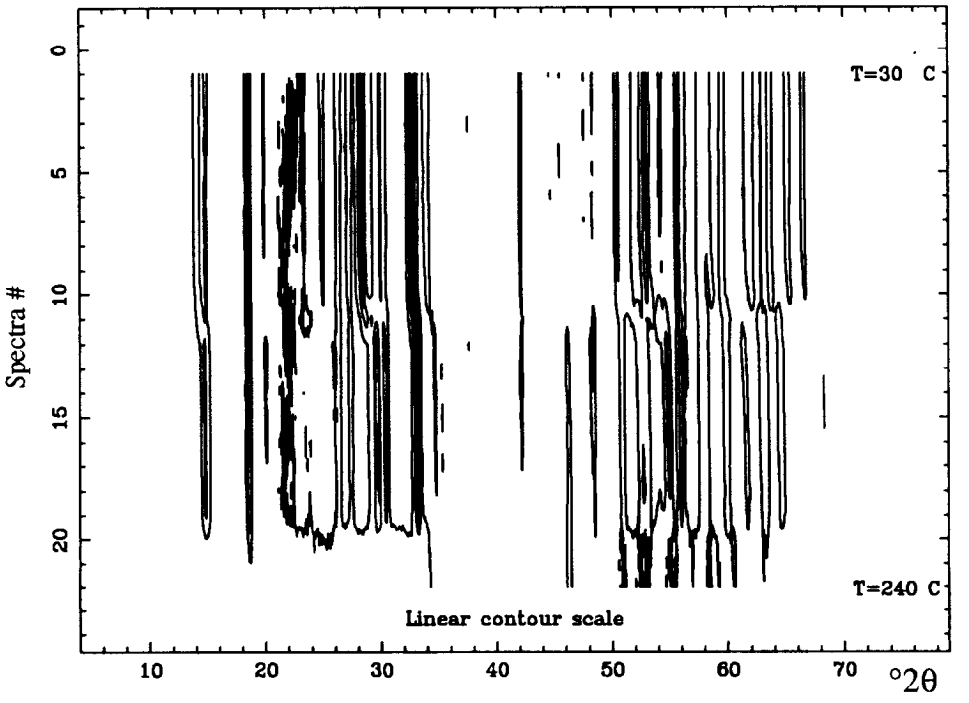

FIG. 8. Contour lines for the powder X-ray thermodiffractogram of Fig. 7.

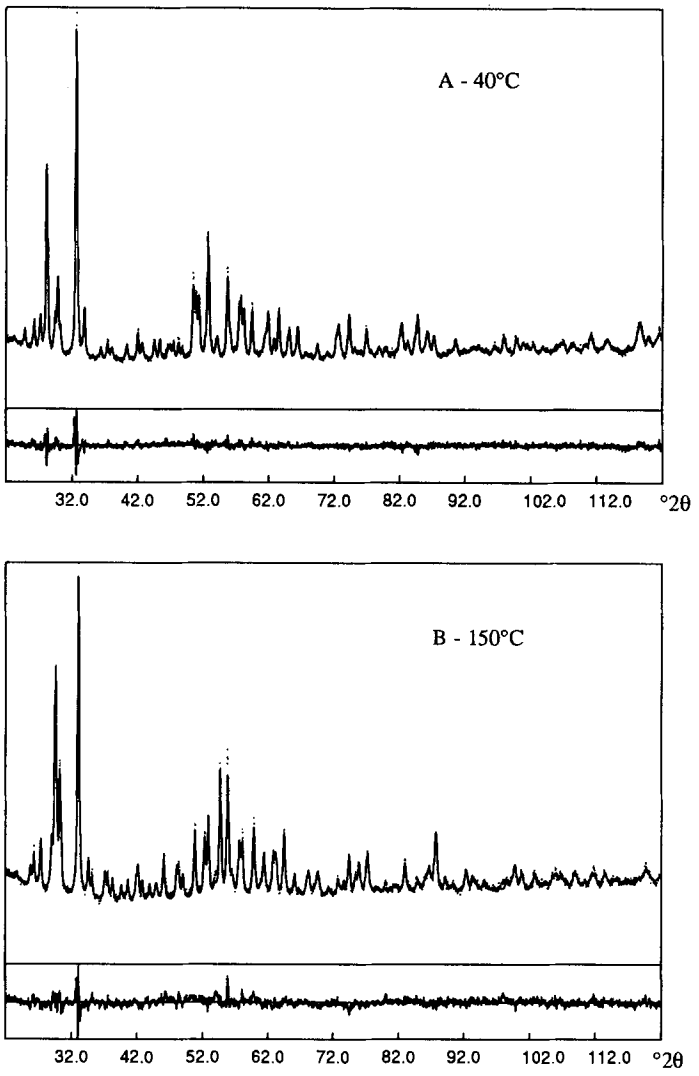

FIG. 9. Example of experimental (···) and calculated (—) powder X-ray patterns (with difference pattern below at the same scale) for $BaZr_2F_{10} \cdot 2H_2O$ at 40°C (Fig. 9A) and at 150°C for $BaZr_2F_{10} \cdot H_2O$ (Fig. 9B).

Structure Description

The structure is drawn in Fig.3; the bidimensional network is built up from infinite F(2)–F(3) corner-sharing in the (001) planes of $[Zr_2F_{14}]^{6-}$ bipolyhedra formed by F(1)–F(1) edge-sharing of two $[ZrF_8]^{4-}$ trigonal dodecaedra. Between each $[Zr_2F_{10}]^{2-}$ layer, Ba^{2+} cations and H_2O molecules ensure the cohesion of the structure; their environment is shown in Fig. 4. This structure is closely related to that of $TlZrF_5$ described by D. Avignant *et al.* (*23*); we observe the same framework built on $[ZrF_8]^{4-}$ polyhedra but the structure is distorted to the monoclinic system (Fig. 5). On the basis of identical volume (two layers for $TlZrF_5$), a direct

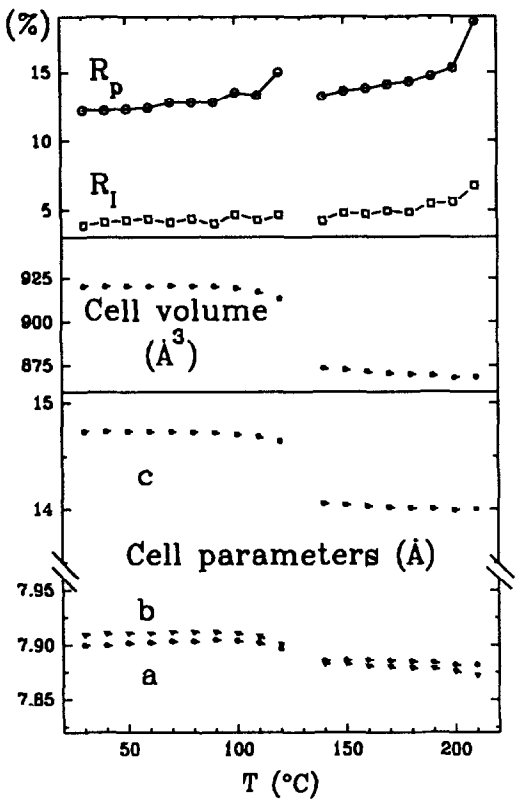

FIG. 10. Variation of the cell parameters, of the cell volume, and of the reliability factors during the Rietveld refinement in the 30–210°C range.

comparison can be made concerning site occupation between each layer (see also Fig. 4):

—Tl half occupies the two types of cavity marked in Fig. 5

—O(1) and Ba fully occupy the *A-type* cavity

—O(2) half occupies the *B-type* cavity.

This leads for the two compounds to the formula:

$$[Tl, \square]\,[Tl, \square]\,Zr_2F_{10}$$
$$[O(2), \square]\,[Ba, O(1)]\,Zr_2F_{10}.$$

Since $BaZr_2F_{10} \cdot 2H_2O$ is synthesized under hydrothermal conditions, some F/OH and/or HF/H_2O exchange could occur; thus we performed a valence bond analysis using the Zachariasen law for Ba–F (*24*) and Zr–F (*25*) bonds and the Brown–Shannon law for Ba–O (*26*). Results are shown Table V; the data are consistent with the proposed formulation and suggest in part a hydrogen bonding scheme. The F(5) valence deficit would be compensated by the bond from a hydrogen atom belonging to the O(1) water molecule; this is confirmed by the O(1)–F(5) short distance (see Table IV); moreover, two F(5) from two adjacent layers are linked by the same O(1) water molecule. Hydrogen bonding involving the O(2) water molecule is not so clear: the nearest anionic neighbors of O(2) are F(4) and O(1); however, the valence deficit on F(4) is weak; also, two barium ions coordinate to O(2), which could easily form long bonds with O(2) lone pairs. Finally, one must remember the static disorder which affects its site.

Thermal Behavior of $BaZr_2F_{10}$, $2H_2O$

The dehydration of $BaZr_2F_{10} \cdot 2H_2O$ has been studied by the TGA technique (TGA 4 system from Perkin–Elmer) and by X-ray thermodiffractometry measurements (it is difficult to prevent a shift between observed temperatures in two such different techniques, which involve different heating rates, thermal exchange areas, etc., leading to nonidentical kinetic characteristics).

The TGA curve of Fig. 6 indicates that dehydration takes place in two steps: the first is clearly apparent near 160°C; a more gradual evolution occurs for the second H_2O molecule up to 300°C; this is consistent with the described crystal chemistry; above 500°C a decomposition process takes place due to ZrF_4 sublimation; at 800°C the residue is BaF_2.

In the second method, we used a Siemens D5000 θ/θ X-ray diffractometer with a position sensitive detector (PSD) and an Anton Parr temperature attachment. The sample is crushed and placed on platinum foil which

TABLE VI

RIETVELD REFINEMENT RESULTS OF 150°C X-RAY SPECTRUM OF $BaZr_2F_{10} \cdot H_2O$

Atom	Site	x	y	z	B (Å)
Ba	4*c*	0.1216(6)	0.0737(6)	¼	3.5(1)
Zr	8*d*	0.3320(6)	0.3354(7)	0.0015(3)	0.6(1)
F(1)	8*d*	−0.010(2)	−0.010(3)	0.080(1)	1.3(2)
F(2)	8*d*	0.069(3)	0.289(4)	0.020(2)	1.3(2)
F(3)	8*d*	0.292(3)	0.054(3)	0.003(1)	1.3(2)
F(4)	8*d*	0.294(3)	0.299(3)	0.153(1)	1.3(2)
F(5)	8*d*	0.256(3)	0.330(3)	0.871(1)	1.3(2)
O(2)	4*c*	0.479(4)	0.030(5)	¼	2.4(9)

Zr polyhedron ⟨Zr–F⟩ = 2.11 Å

Zr	F(5)	F(3)	F(2)	F(2)	F(1)	F(4)	F(1)	F(3)
F(5)	**1.92(2)**	2.53(4)	2.58(3)	3.37(3)	3.74(2)	3.97(4)	2.47(3)	2.87(3)
F(3)	80.5(0.8)	**1.99(2)**	2.38(4)	3.94(4)	2.54(3)	3.06(3)	2.66(3)	4.00(4)
F(2)	79.1(1.0)	71.0(1.1)	**2.12(2)**	4.00(4)	3.84(3)	2.58(3)	4.07(3)	2.56(4)
F(2)	112.5(1.0)	146.8(1.1)	139.8(0.6)	**2.13(3)**	2.57(4)	2.93(3)	2.65(4)	2.52(4)
F(1)	132.7(0.9)	75.4(0.8)	127.8(0.9)	73.7(1.0)	**2.16(2)**	2.49(4)	2.25(3)	4.06(3)
F(4)	152.6(1.0)	94.8(0.8)	73.9(1.0)	86.2(1.0)	70.4(0.8)	**2.17(2)**	3.98(2)	2.85(3)
F(1)	73.6(0.8)	79.3(0.8)	142.4(1.0)	75.8(1.0)	62.4(0.7)	132.4(0.7)	**2.18(2)**	4.01(3)
F(3)	86.7(0.8)	142.3(0.4)	71.9(1.1)	70.6(1.0)	135.0(0.8)	80.7(0.7)	130.5(0.8)	**2.24(2)**

Ba environment ⟨Ba–*X*⟩ = 2.84 Å

2×	Ba–F(4)	2.62(2)
2×	Ba–F(1)	2.69(1)
2×	Ba–F(5)	2.74(2)
	Ba–O(2)	2.84(3)
2×	Ba–F(4)	3.08(2)
	Ba–O(2)	3.31(4)

O(2) environment ⟨O(2)–*X*⟩ = 3.02 Å

	O(2)–Ba	2.84(3)
2×	O(2)–F(4)	2.90(4)
2×	O(2)–F(4)	2.98(4)
2×	O(2)–F(5)	3.14(4)
	O(2)–Ba	3.32(4)

Note. Pnam orthorhombic cell (Å): a = 7.8859(6), b = 7.8825(6), c = 14.0381(8), η = 0.84(1), U = 0.14(3), V = −0.03(3), W = 0.098(8), R_I = 0.048, R_p = 0.136. Sites, atomic coordinates, isotropic temperature factors, main distances (Å), and angles (°) are listed, wtih e.s.d.'s in parentheses.

serves as a heating source; the chamber is pumped under vacuum and then filled with dry helium; a light flow of helium is maintained during the experiment to improve thermal conductivity. The conditions for X-ray spectra recording are as follows:

—radiation Co$K\alpha$

—fast scan with step time = 20 s and 2θ step size = 0.032° in the 2θ range: 10°–130°

—temperature range 30–240°C by 10°C steps and a slewing speed of 0.1°C/s.

Figure 7 shows a part of the set of raw spectra; the contour plot is shown in Fig. 8. It must be emphasized that the experiment is not time resolved; a full pattern recording for the series shown in Fig. 7 takes 24 hr. Also, the sample probably does not have a homogeneous temperature profile.

The Rietveld refinements of all the spectra in the 30–220°C range (Fig. 9) give convergent results from which are extracted the reliability factors, the cell volume, and the cell parameter variations shown in Fig. 10. Examination of these figures, combined with the TGA results, permits one to distinguish three temperature domains:

—up to 120°C, the crystal structure of $BaZr_2F_{10} \cdot 2H_2O$ undergoes only a slight thermal expansion.

—near 130°C a transitional behavior appears which could correspond to the loss of the first H_2O molecule. The refinement of

this spectrum becomes problematical; neither R nor cell parameters can be obtained, probably because the pattern represents a mixture of the two barium fluorozirconate hydrates. This dehydration process is reversible if the sample is not heated above 200°C, according to the scheme:

$$BaZr_2F_{10} \cdot 2H_2O \leftrightarrows BaZr_2F_{10} \cdot H_2O + H_2O.$$

—from 140 to 210°C the initial crystal structure is maintained but with only one H_2O molecule; the main effect of eliminating the O(1) water molecule is to decrease the c cell parameter (corresponding to a decrease in the $[Zr_2F_{10}]^{2-}$ interlayer distance); at this point, $BaZr_2F_{10} \cdot H_2O$ and $TlZrF_5$ probably have the same average atomic configuration:

$$[Tl, \square]\,[Tl, \square]\,Zr_2F_{10}$$
$$[O(2), \square]\,[Ba, \square]\,Zr_2F_{10}.$$

Table VI gives, as an example, the results of the refinement of the 150°C spectrum with coordinates and main interatomic distances for $BaZr_2F_{10} \cdot H_2O$; the remaining H_2O molecule corresponds to the O(2) molecule in $BaZr_2F_{10} \cdot 2H_2O$. In fact, the continuous loss of the second H_2O molecule, as suggested by the TGA curve, was confirmed by tests of refinement of either the thermal vibration or the occupancy factor of O(2) in the 150–210°C range with a clear increase of B or decrease of the occupancy.

Above 210°C the amorphous phase which appears could correspond to the collapse of the structure when the last portion of the $H_2O(2)$ molecules is eliminated.

Conclusion

$BaZr_2F_{10} \cdot 2H_2O$ is the principal phase formed by action of aqueous HCl on mixtures of BaF_2–ZrF_4 or on ZBLAN glasses. The structure determination establishes edge-sharing of $[ZrF_8]^{2-}$ polyhedra (already encountered in α-ZrF_4 (*27*), and also in β-$BaZr_2F_{10}$ (*4*), but for $[ZrF_7]^{3-}$ polyhedra in a tridimensional network) building $[Zr_2F_{14}]^{6-}$ bipolyhedra linked together by corners to form infinite $[Zr_2F_{10}]^{2-}$ layers separated by Ba atoms and H_2O molecules. The dehydration process is reversible for the first H_2O molecule if the sample is not heated over 200°C and the original crystal structure is maintained up to 200°C, when the last H_2O molecules are eliminated.

References

1. J. P. Laval, B. Frit, and B. Gaudreau, *Rev. Chim. Miner.* **16,** 509 (1979).
2. J. P. Laval, R. Papiernik, and B. Frit, *Acta Crystallogr. B* **34,** 1070 (1978).
3. J. P. Laval, D. Mercurio-Lavaud, and B. Gaudreau, *Rev. Chim. Miner.* **11,** 742 (1974).
4. J. P. Laval, B. Frit, and J. Lucas, *J. Solid State Chem.* **72,** 181 (1988).
5. J. M. Parker, G. N. Ainsworth, A. B. Seddon, and A. Clare, *Phys. Chem. Glasses,* **27**(6), 219 (1986).
6. J. M. Parker, A. B. Seddon, and A. G. Clare, *Phys. Chem. Glasses,* **28**(1), 4 (1987).
7. A. B. Seddon, D. L. Williams, and A. G. Clare, *Phys. Chem. Glasses,* **31**(2), 64 (1990).
8. B. Boulard, A. Le Bail, J. P. Laval, and C. Jacoboni, *J. Phys. (Les Ulis, Fr.)* **47**(2), 791 (1986).
9. A. Le Bail and A. M. Mercier, submitted for publication.
10. G. M. Sheldrick, C. Kruger, and R. Goddard (Eds.) "Crystallographic Computing 3: Data Collection, Structure Determination, Proteins and Databases," pp 184–189, Oxford Univ. Press (Clarendon), London/New York (1985).
11. "International Tables for X-Ray Crystallography," Vol. 4, Kynoch Press, Birmingham (1974).
12. T. Suzuki, *Acta Cryst.* **13,** 279 (1960).
13. G. M. Sheldrick, "SHELX; A Program for Crystal Structure Determination," University of Cambridge (1976).
14. A. Le Bail, unpublished TMACLE program.
15. A. Le Bail, Y. Gao, and C. Jacoboni, *Eur. J. Solid State Inorg. Chem.* **26,** 281 (1989).
16. A. Hemon, A. Le Bail, and G. Courbion, *J. Solid State Chem.* **81,** 299 (1989).
17. A. Le Bail, Y. Gao, J. L. Fourquet, and C. Jacoboni, *Mater. Res. Bull.* **25,** 831 (1990).
18. M. C. Moron, A. Le Bail, and J. Pons, *J. Solid State Chem.* **88,** 498 (1990).

19. W. C. HAMILTON, *Acta Crystallogr.* **12,** 609 (1959).
20. H. M. RIETVELD, *J. Appl. Crystallogr.* **2,** 65 (1969).
21. D. B. WILES, A. SAKTHIVEL, AND R. A. YOUNG, Program DBW3.2S (1987).
22. D. B. WILES AND R. A. YOUNG, *J. Appl. Crystallogr.* **14,** 149 (1981).
23. D. AVIGNANT, I. MANSOURI, R. CHEVALLIER, AND J. COUSSEINS, *J. Solid State Chem.* **38,** 121 (1981).
24. G. FEREY, M. LEBLANC, A. DE KOZAK, M. SAMOUEL, AND J. PANNETIER, *J. Solid State Chem.* **56,** 288 (1985).
25. I. MANSOURI AND D. AVIGNANT, *J. Solid State Chem.* **51,** 91 (1984).
26. I. D. BROWN, *in* "Structure and Bonding in Crystals" (M. A. O'Keefe and A. Navrotsky, Eds.), Vol. 2, pp. 1–30, Academic Press, New York (1981).
27. R. PAPIERNIK, D. MERCURIO, AND B. FRIT, *Acta Crystallogr. B* **38,** 2347 (1982).